Analytica Chimica Acta xxx (2018) 1–8

Contents lists available at ScienceDirect

Analytica Chimica Acta

journal homepage: www.elsevier.com/locate/aca

# Rapid and low-cost strategy for detecting genome-editing induced deletion: A single-copy case

Nan Cheng [a, 1], Qin Wang [b, 1], Ying Shang [c], Yuancong Xu [a], Kunlun Huang [a, d], Zhansen Yang [a], Dengke Pan [e], Wentao Xu [a, d, *], Yunbo Luo [a, d, **]

[a] Beijing Advanced Innovation Center for Food Nutrition and Human Health, College of Food Science & Nutritional Engineering, China Agricultural University, Beijing, 100083, China
[b] The Institute of Plant Quarantine, Chinese Academy of Inspection and Quarantine, Beijing, 100029, China
[c] Yunnan Institute of Food Safety, Kunming University of Science and Technology, Kunming, Yunnan, 650500, China
[d] Key Laboratory of Safety Assessment of Genetically Modified Organism (Food Safety), Ministry of Agriculture, Beijing, 100083, China
[e] Key Laboratory of Farm Animal Genetic Resource and Germplasm Innovation, Ministry of Agriculture, Institute of Animal Science, Chinese Academy of Agricultural Sciences, Beijing, 100193, China

## HIGHLIGHTS

- A rapid and low-cost strategy for detecting genome-editing induced deletion was developed.
- A rapid-MLPA was first introduced to the LFNAB system.
- The entire detection process could be shortened to 120 min without any large-scale instruments.
- The assay demonstrates at least 100-fold less assay cost compared with current gold standard.
- The method shows remarkable potential in regards to international trade, transparency, and freedom of choice.

## GRAPHICAL ABSTRACT

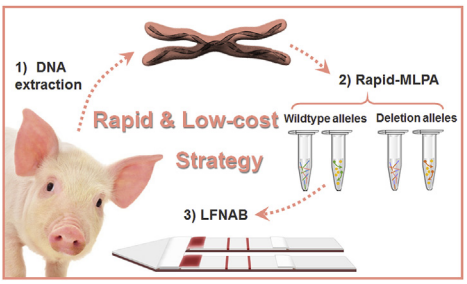


## ARTICLE INFO

*Article history:*
Received 25 December 2017
Received in revised form
12 February 2018
Accepted 19 February 2018
Available online xxx

*Keywords:*
Genome-editing deletion
Single-copy case

## ABSTRACT

Genome editing techniques have been implemented in human daily lives, which has created a high demand for the development of new gene-edited product analysis methods. Conventional assays are time-consuming, labor-intensive, and costly. This paper proposes a rapid and low-cost strategy for detecting genome-editing induced deletion which works by integrating rapid-multiplex ligation-dependent probe amplification (MLPA) with a dual-lateral flow nucleic acid biosensor (LFNAB) cascade in a single-copy case. A rapid-MLPA was first introduced to the LFNAB system as a replacement for the conventional PCR for enhanced specificity and accuracy. A dual-LFNAB was applied for the detection of genome-editing induced deletion without any additional instrumentation or complex operation. After optimization, we achieved the specific detection of wildtype alleles and deletion alleles in spiked

* Corresponding author. Beijing Advanced Innovation Center for Food Nutrition and Human Health, College of Food Science & Nutritional Engineering, China Agricultural University, Beijing, 100083, China.
** Corresponding author. Beijing Advanced Innovation Center for Food Nutrition and Human Health, College of Food Science & Nutritional Engineering, China Agricultural University, Beijing, 100083, China.
*E-mail addresses:* xuwentao@cau.edu.cn (W. Xu), lyb@cau.edu.cn (Y. Luo).
[1] These authors contribute equally to this work.

https://doi.org/10.1016/j.aca.2018.02.060
0003-2670/

Dual-lateral flow nucleic acid biosensor
Rapid-multiplex ligation-dependent probe amplification
WUZHISHAN pig

samples with a detection limit of 0.4 fM, which is comparable to that of electrophoresis-based detection assays and fluorescent biosensors. To confirm the validity and feasibility of our strategy, we assayed two pork samples from two WUZHISHAN pigs successfully. By comparing the detection results from next-generation sequencing analysis, we found that the proposed cascade demonstrates at least 20-fold shorter assay time and at least 100-fold less assay cost. To this effect, the proposed method is a rapid and low-cost solution to sample-to-answer detection of genome-editing induced deletion and shows remarkable potential in regards to international trade, transparency, and freedom of choice.



## 1. Introduction

Recent advancements in genome editing techniques such as ZFNs [1], TALENs [2], and CRISPR-Cas9 [3] are revolutionizing our ability to conduct efficient and directed alterations of the eukaryotic genome. These include the functional knockout of endogenous genes or alleles, the targeted induction or correction of specific mutations or other polymorphisms, and precise modeling of genetic contributions to normal cellular function [4]. The ability to precisely modify the genome in a targeted fashion has already had a huge impact on basic scientific research, industrial biotechnology, and especially medicine. At present, genome editing techniques have been implemented in a number of food products under permissive regulatory conditions [5]. Gene-edited crops and gene-edited mushrooms have been free to enter the US market and be sold without oversight by the US Department of Agriculture (USDA) [6,7]. In other words, the transparency of international trade among countries and the freedom of choice for consumers have together created a demand for new gene-edited product analysis methods.

Previous studies demonstrated that next generation sequencing combined with PCR amplification of targeted regions represents the gold standard for quantitative determination of genome-editing induced mutation [8]. This process, unfortunately, takes two full days, is specific to particular sequencing platforms, and is complicated by the laborious procedures [9]. Research teams led by Miyaoka and Findlay have optimized this detection method by using digital PCR technology to further improve its efficiency [8,10]. Although they did successfully detect rare genome-editing events, these methods are still laborious and relatively expensive. The gel-based methods for genome-editing induced detection, such as polymerase chain reaction (PCR)/restriction enzyme (RE) assay and T7 endonuclease I (T7E1) assay, are cost-effective but still require highly complex operation including pouring the agarose gel, loading samples, running the agarose gel, and analyzing the gel [11]. A low-cost, truly convenient genome editing product detection method is paramount to moving forward with new projects in this field.

Multiplex ligation-dependent probe amplification (MLPA) has emerged as an alternative to standard PCR amplification for DNA sequence detection [12]. The method is based on the multiplex amplification of ligated probes, and exhibits better accuracy, stronger robustness, and higher multiplex ability. Commercial MLPA kits have been updated constantly and are now rather advanced (http://www.mrc-holland.com/), but come with long turn-around time [13,14] which hinders their wider application significantly. There is urgent demand for newer, more rapid MLPA techniques.

There are also limitations to the product detection technologies of MLPA. Conventional MLPA is dependent on the length-based discrimination of products, which requires electrophoresis-based assays such as capillary electrophoresis and sequencing gel electrophoresis [15,16]. A main drawback is the different sizes of fragments holding different efficiencies within a multiple reaction, which affects the determination of relative amounts [14]. In recent years, biosensor-based assays based on uniform-size amplification products have been developed to overcome this limitation, including the electrochemical biosensor and fluorescent biosensor [17–19].

Accordingly, lateral flow nucleic acid biosensor (LFNAB) is a significant and powerful tool in analytical and detection fields due to its simple operation, high sensitivity, and low cost [20–22]. In our previous work, we successfully analyzed DNA methylations via LFNAB and obtained a relatively low detection limit [22]. We also successfully fabricated a multi-branched LFNAB for multiplex nucleic acid detection, and applications such as stacked genetically modified soybeans identification and microRNAs determination have been reported [23,24]. This methodology seems to be readily adaptable to MLPA products and shows interesting potential for the detection of genome-editing products. The utility and performance of such assays have not yet been thoroughly assessed, however.

In this paper, we report a rapid, sensitive, and inexpensive strategy for genome-editing product detection on the basis of a single-copy case. We first introduced rapid-MLPA to the LFNAB system as a substitute for conventional PCR for better specificity and accuracy. A dual-LFNAB was then applied to detect genome-editing induced deletion without necessitating any additional instrumentation or complex operation. As proof-of-concept, we used a single-copy 90-bp length dsDNA from *GGTA1* knockout pig as a model sequence; the model reflects the crucial regulatory roles in pig-to-human xenotransplantation [25,26]. The WUZHISHAN pig with one-base deletion from the wildtype was produced via TALENS system [25], but the proposed LFNAB can serve as a platform for the detection of genome-editing products from an array of approaches and protocols. As discussed below, the rapid-MLPA and dual-LFNAB cascade allowed us to identify both homozygous and heterozygous gene deletion easily and quickly.

## 2. Materials and methods

### 2.1. Animals

The genome-edited WUZHISHAN pig used in this study was generated by TALENS (the Institute of Plant Quarantine, Chinese Academy of Inspection and Quarantine, Beijing, China). The wild-type WUZHISHAN pig we used was also provided by the Institute of Plant Quarantine, Chinese Academy of Inspection and Quarantine.

### 2.2. Materials

Chloroauric acid tetrahydrate ($HAuCl_4 \cdot 4H_2O$), NaCl, trisodium citrate, Tween-20, bovine serum albumin (BSA), phosphate buffered saline (PBS, pH 7.4, 0.01 M), sodium chloride–sodium citrate (SSC) buffer (20 concentrate, pH 7.0), Tris-Hcl buffer (pH 7.4, 10 mM), and borate buffer (BB, pH 9.0, 0.1 M) were purchased from

Please cite this article in press as: N. Cheng, et al., Rapid and low-cost strategy for detecting genome-editing induced deletion: A single-copy case, Analytica Chimica Acta (2018), https://doi.org/10.1016/j.aca.2018.02.060

Sigma Chemical Company (St. Louis, MO, USA). The anti-biotin antibody, anti-FITC antibody, anti-digoxin antibody, and goat anti-mouse IgG we used were purchased from Abcam Inc. (Cambridge, MA, USA). Backing cards (HF000MC100), glass fiber sample pads (CFSP001700), conjugation pads (GFCP000800), nitrocellulose membranes (135s), and absorbent pads (CFSP001700) were purchased from Millipore (Bedford, MA, USA). Double distilled water (ddwater) was used throughout the experiments.

### 2.3. Rapid-MLPA procedure

#### 2.3.1. Design of rapid-MLPA probes

The probes were designed using ABI PRISM Primer Express version 2.0 software (Applied Biosystems, Foster City, CA, USA) as presented in Fig. S1. Each probe consisted of a target-specific sequence and common sequence. The annealing temperatures of the target-specific sequence on the probes and template strongly influenced the efficiency and specificity of our method, especially during the first ligation reaction. Left and right hybridizing probes were, minimally, 17 nucleotides long and had a melting temperature ($T_m$) of approximately 60 °C, which is consistent with the optimum reaction temperature of the ligase-65. Hence, the target-specific sequences hybridized with the templates first and then ligated during thermal cycling. Each common sequence on the probe was aligned with BLAST (https://blast.ncbi.nlm.nih.gov/Blast.cgi) against the WUZHISHAN pig genome sequence (GENBANK: AJKK01000000). No significant homology was found in any of the four common sequences. All the oligonucleotides used in this study (Table S1) were synthesized by Takara (Dalian, China).

#### 2.3.2. Rapid-MLPA assays

Hybridization and ligation reactions were performed in 0.5-mL PCR reaction vessels with a thermocycler (Applied Biosystems). An initial incubation of 5 min at 98 °C was followed by the addition of 1.5 μL of a mixture containing 0.75 μL MLPA Buffer (MRC-Holland, Amsterdam, the Netherlands) and 0.75 μL of a solution containing 3 fmol of each probe (left and right). The mixture was incubated at 95 °C for 60 s to denature the probes, after which hybridization took place at 60 °C for 5 min. The ligation of MLPA probes was then performed by adding 32 μL of a mixture containing 3 μL ligase buffer A (MRC-Holland, Amsterdam, the Netherlands), 3 μL Ligase Buffer B (MRC-Holland, Amsterdam, the Netherlands), 1 μL Ligase-65 (MRC-Holland), and 25 μL of water. Ligation was performed for 7 min at 54 °C followed by an incubation of 5 min at 98 °C. The PCR mix used for ligation product amplification (25 μL volume) contained 10 × rTaq buffer with 1 U of rTaq polymerase, 12.5 μmol of each dNTP (Takara), 1 μL of each primer (10 nM), and 2 μL of template from the ligation mix. DNA denaturation and polymerase activation at 95 °C for 5 min were followed by 35 amplification cycles at 95 °C for 30 s, 60 °C for 30 s, and 72 °C for 60 s, with a final step of 5 min at 72 °C. The reaction mixtures were then cooled to 4 °C.

For real sample detection, genomic DNA was extracted from the pig samples using Qiagen DNeasy® Tissue Kits (Qiagen, Hilden, Germany). The genomic DNA was found to be suitable as rapid-MLPA templates. Other operations were conducted in the same manner as the general procedure.

### 2.4. Dual-LFNAB procedure

#### 2.4.1. Fabrication of AuNPs-antibody conjugate

AuNPs-antibody conjugates were synthesized following a previously published method with slight modification [22]. Briefly, a 50 mL aqueous solution of $2.4 \times 10^{-4}$ M $HAuCl_4$ was heated to boiling and 1.67 mL of 1% trisodium citrate was added. The boiling solution was stirred for another 30 min, then stored at 4 °C until use. AuNPs-antibody conjugate reactions were conducted by adding 5 μL of 10 mM anti-biotin antibody and 20 μL of 10% BSA solution into 1 mL of AuNPs solution (pH 9.0 with borate buffer solution), followed by incubation at room temperature with periodic agitation for 1 h. The solution was then centrifuged at 13,000 × g for 15 min. Two phases were obtained: a clear-to-pink supernatant of unbound antibodies and a dark red, loosely packed sediment of the anti-biotin-AuNPs conjugates. The resulting AuNPs-antibody conjugates were stored at 4 °C until further use.

#### 2.4.2. Preparation of the dual-LFNAB

The dual-LFIA was consisted of a triangle-shape sample pad, two conjugate pads, two nitrocellulose membranes, two absorbent pads, and an interoperable backing. The sample pad was made from glass fiber and saturated with 1 × PBS containing 1% BSA and 0.25% Tween-20, then dried overnight at room temperature. Two test lines and two control lines were prepared by dispensing mouse anti-FITC polyclonal antibody (or mouse anti-digoxin polyclonal antibody) solution (1.0 mg/mL) and goat anti-mouse IgG antibody solution (1 mg/mL) at different locations on the nitrocellulose membrane with a BioDot BioJet BJQ 3000 dispenser (Irvine, CA). The distance between lines was approximately 1 cm. The nitrocellulose membranes were then dried overnight at 37 °C and stored at 4 °C. The conjugate pads and absorbent pads were assembled on backing with an overlap of approximately 1–2 mm. Single LFNABs were cut at a width of 4 mm using a Bio-Dot Paper Cutter module CM4000 (Irvine, CA). Finally, two LFNABs with different test lines were assembled together on the triangle-shape sample pad. The assembled dual-LFIA was either used immediately or stored under dry conditions at room temperature until further testing.

### 2.5. Detection of genome-editing induced deletion

Following rapid-MLPA, 75 μL of running buffer was mixed with 25 μL of the amplified product solution, then the mixture was applied to the sample pad of the dual-LFNAB and migrated upward by capillary force. The lines were evaluated visually after 4 min; naked-eye detection was performed simply by observing color changes in the two test lines. The quantitative detection was performed by recording the peak area of each line in ImageJ software (http://rsb.info.nih.gov/ij). The entire detection process was truncated to 120 min without any large-scale instrumentation.

### 2.6. Other techniques for characterization

Agarose gel electrophoresis were performed using 2% agarose stained with ethidium bromide. The amplification products for next generation sequencing were sent to Sangon Biotech Company (Shanghai, China). X-ray diffraction (XRD) pattern was performed on a D8 ADVANCE X-ray diffractometer (Brucker AXS, Karlsruhe, Germany). The morphologies of the nanomaterial were characterized by transmission electron microscopy (TEM) on a Philips CM200 UT (Field Emission Instruments, USA) at an accelerating voltage of 40 KV. The zeta potential was measured using a zeta potential analyser (Brookhaven Instruments Co, USA). The UV-vis spectroscopy was recorded on a spectrophotometer (QuantaMasterTM40) under the external excitation of a 250 mW 980 nm laser diode (RGB Laser systems). Fourier transform infrared (FTIR) spectra was recorded in the range of 400–4000 $cm^{-1}$ with 0.5–4 $cm^{-1}$ resolution using a Tensor 27 FTIR spectrophotometer. X ray photoelectron spectral (XPS) analysis was performed with a Surface Science Instrument SSX-100. All measurements were performed at room temperature.

Please cite this article in press as: N. Cheng, et al., Rapid and low-cost strategy for detecting genome-editing induced deletion: A single-copy case, Analytica Chimica Acta (2018), https://doi.org/10.1016/j.aca.2018.02.060

## 3. Results and discussion

### 3.1. Principle

Our strategy for detecting genome-editing induced deletion is illustrated in Scheme 1. The deletion occurred on the pig *GGTA1* exon 4 region (Scheme 1A). After DNA extraction, we used the cascade based on rapid-MLPA and dual-LFNAB for rapid and low-cost determination. Rapid-MLPA was used to generate numerous double tags attached to duplex DNA products (Scheme 1B), which involves amplification of the wildtype alleles and deletion alleles, respectively. The solution for hybridization and ligation (step 1) consists of a left probe, a right probe, and ligase-65. The left probe and right probe partially hybridize to the target sequence. In the presence of a complementary target sequence, the two probes hybridize next to each other and are subsequently ligated followed by conventional polymerase chain reaction (PCR) with two tag-labeled primers (step 2). This involves a pair of FITC-primer and biotin-primer for wildtype alleles and a pair of digoxin-primer and biotin-primer for deletion alleles. Finally, the duplex DNA with biotin- and FITC- (or digoxin-) attached are produced as a rapid-MLPA product. In the absence of a complementary target sequence, ligation does not occur and amplification of the two rapid-MLPA probes does not take place.

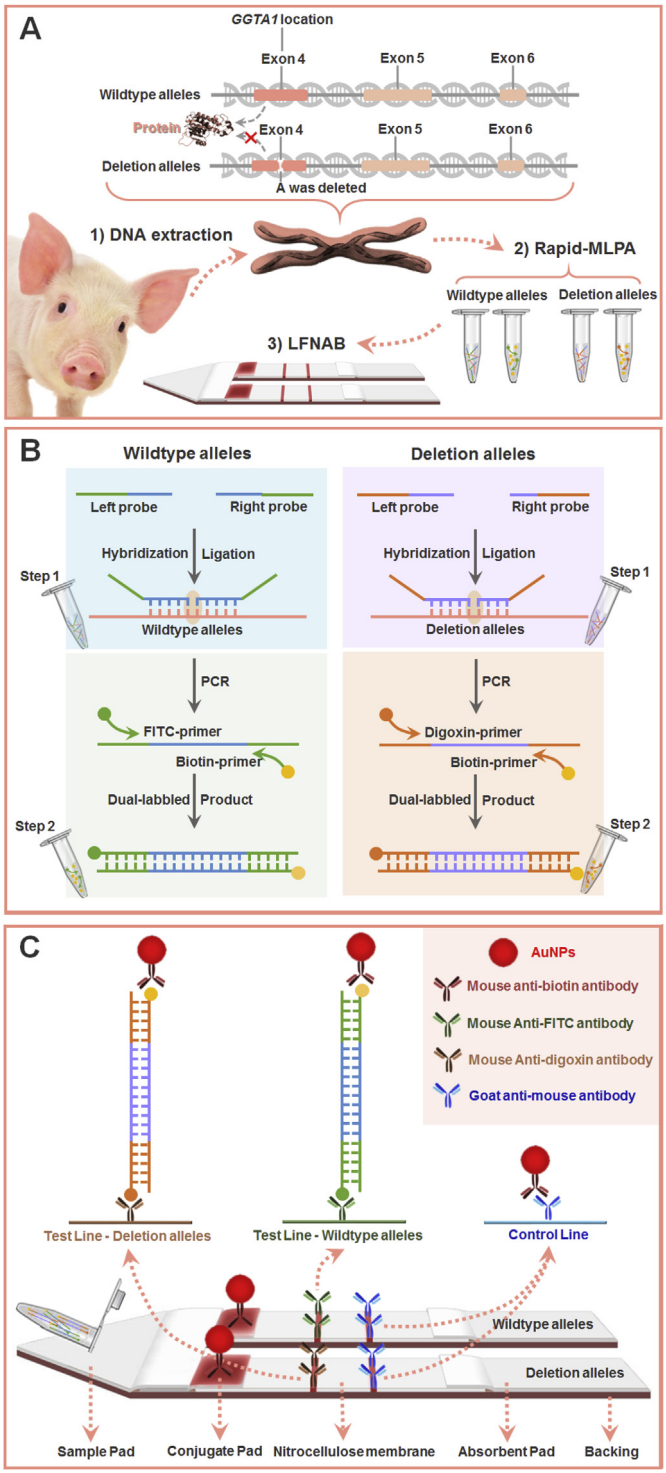


**Scheme 1.** Rapid-MLPA and dual-LFNAB cascade for detecting genome-editing induced deletion. A) Brief summary of work flow; B) Rapid-MLPA procedure; C) Dual-LFNAB procedure.

The parallel design of our dual-LFNAB is the key to obtain high sensitivity and specificity, which is based on careful consideration of cross-reactivity and the limitation of Washburn's theory [27]. The principle of the dual-LFNAB is based on a sandwich reaction (Scheme 1C). To run the reaction, mouse anti-biotin antibody-modified AuNPs conjugates are pre-loaded on the two conjugate pads. Mouse anti-FITC antibody and mouse anti-digoxin antibody are immobilized on a nitrocellulose membrane to form the test lines for wildtype alleles and deletion alleles, respectively. Goat anti-mouse antibody, which works against mouse anti-biotin antibody, is immobilized on the two control lines.

In our experiment, we applied sample solutions containing rapid-MLPA products onto a sample pad. The solution then migrated due to capillary action, and the hybridization reactions among rapid-MLPA products, mouse anti-biotin antibody-modified AuNPs conjugates, and corresponding antibodies were immobilized on the test line, forming a sandwich construction. In a typical assay, when wildtype alleles or homozygous deletion alleles are present in the sample, only one visible red line can be observed on one of the test lines (Figs. S2A and S2B). If genome-editing induced deletion is heterozygous, two red lines can form (Fig. S2C). When we applied a negative control sample onto the sample pad, no red lines were observed on the test lines (Fig. S2D). Once the solution passed through the control lines, the excess mouse anti-biotin antibody-modified AuNPs conjugates were captured by the secondary antibody, thus two additional red lines appeared; this indicated that the dual-LFNAB worked properly and that signals on the test lines were reliable.

### 3.2. Characterization

#### 3.2.1. Rapid-MLPA

Agarose gel electrophoresis was conducted to character the feasibility of rapid-MLPA. We first detected the wildtype alleles and deletion alleles individually, which can be viewed as a wildtype gene sample and homozygous deletion gene sample. Then, wildtype alleles were mixed with equal volume deletion alleles to simulate a heterozygous deletion gene sample. After rapid-MLPA, the products were detected by agarose gel electrophoresis, which showed clear bright lines for all positive samples and confirmed the feasibility of rapid-MLPA (Fig. S3). However, agarose gel electrophoresis cannot separate the rapid-MLPA products derived from wildtype alleles and deletion alleles due to their same length.

#### 3.2.2. Nanoparticles

It is important to know the exact crystal structure of the AuNPs, which can be obtained by measuring the XRD spectrum. As shown in Fig. S4, the distinct XRD peaks were indexed to the (111), (200),

Please cite this article in press as: N. Cheng, et al., Rapid and low-cost strategy for detecting genome-editing induced deletion: A single-copy case, Analytica Chimica Acta (2018), https://doi.org/10.1016/j.aca.2018.02.060

(220) and (311) planes of a face centered cubic (fcc) structure (JCPDS 04-0783) revealing that the synthesized AuNPs are composed of pure crystalline gold. We collected TEM images to investigate the morphology of AuNPs. As shown in Fig. 1A, the as-synthesized AuNPs were well dispersed and approximately 23 nm in size. Fig. 1B showed a bright circle around AuNPs, which indicatd the functionalization of antibodies. To further verify the successful conjugation of antibodies, we measured the zeta potential and UV-vis absorption spectra of gold nanoparticles before and after modification. As shown in Fig. 1C, the zeta potential decreased from −34.6 to −27.5 mV for anti-biotin antibody conjugations, which indicated successful antibody modification. As shown in Fig. 1D, a well-defined peak with maximum absorption wavelength of 520 nm for AuNPs and 524 nm for AuNPs-antibody conjugates were obtained which also confirmed successful antibody functionalization. As shown in Fig. 1E–F, a small peak around 1550 $cm^{-1}$ and 2960 $cm^{-1}$ corresponding to amide group and CH group were observed after antibody modification in the FTIR spectra, which also confirmed antibody functionalization successfully. In addition, electronic state and chemical characterization have been carried out by XPS techniques. In Fig. S5, the sample of AuNPs-antibody conjugates showed a high peak at ~398 eV, which corresponds to nitrogen present in the sample from anti-biotin antibodies and BSA. It's clear to confirm that the anti-biotin antibodies and BSA have been loaded on AuNPs successfully.

### 3.3. Optimization

To obtain the shortest analysis time and the optimal analytical performance of the rapid-MLPA and dual-LFNAB cascade, we employed wildtype alleles (1 pM) as a target to optimize the reaction steps. Based on our previous work [15], the hybridization time, ligation time, and PCR cycles were optimized with respect to agarose gel electrophoresis in this system (Fig. S6). We found that the intensity of target bands remained stable with increasing hybridization time from 5 min to 35 min (Fig. S6A). The brightest band was obtained under 7 min for ligation (Fig. S6B) and 35 cycles for PCR (Fig. S6C), thus marking the appropriate time for ligation and optimized amplification cycles. The hybridization between target and probes (left and right) was incubated for 5 min, the ligation between left probe and right probe was incubated for 7 min, and the cycle number for PCR was selected to be 35 in all subsequent tests accordingly.

Considering that the accumulation of AuNPs on the lines can

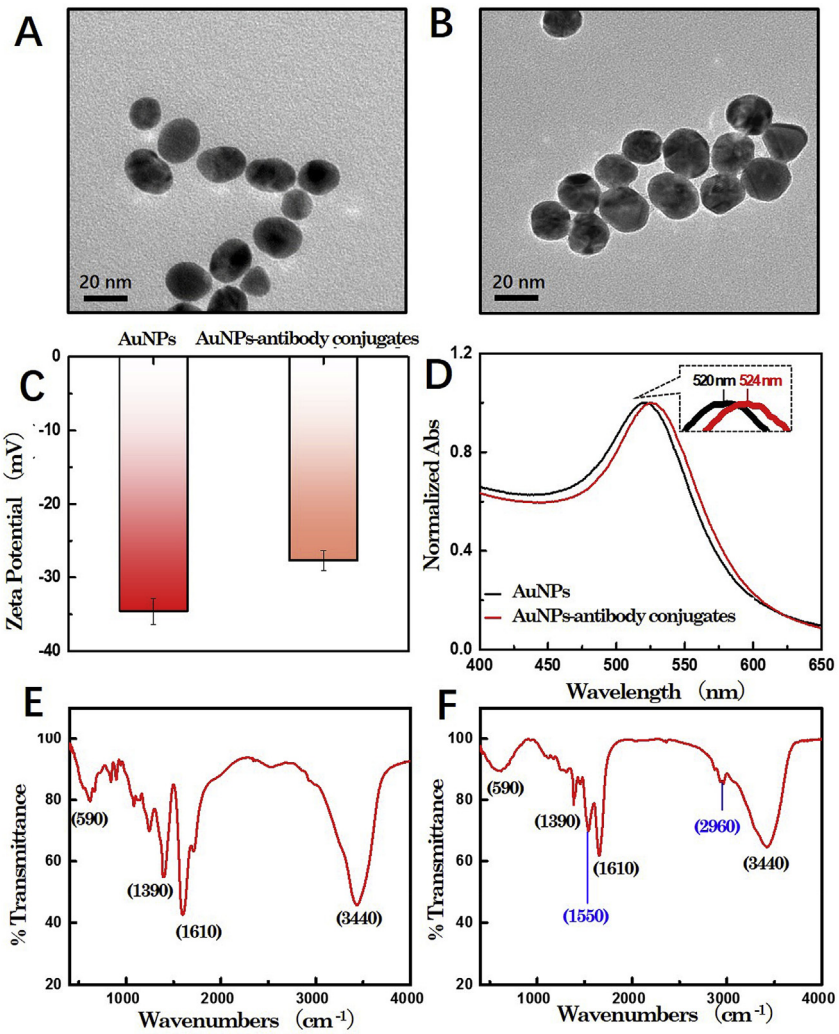


**Fig. 1.** Characterization of AuNPs and AuNPs-antibody conjugates. (A) TEM image of AuNPs; (B) TEM image of AuNPs-antibody conjugates; (C) Zeta potential of AuNPs before and after antibody modification; (D) UV-vis absorption spectra of AuNPs before and after antibody modification; (E) FTIR spectra of AuNPs; (F) FTIR spectra of AuNPs-antibody conjugates. Concentration of Au-NPs: 2.5 nM.

Please cite this article in press as: N. Cheng, et al., Rapid and low-cost strategy for detecting genome-editing induced deletion: A single-copy case, Analytica Chimica Acta (2018), https://doi.org/10.1016/j.aca.2018.02.060

significantly affect the responses of the dual-LFNAB, various factors were systematically investigated including the concentration of AuNPs, AuNPs-antibody conjugate quantities, accumulation time, and the type of running buffer (Fig. 2). AuNPs with different concentrations were prepared by dilution from stock solutions at different folds. As depicted in Fig. 2A, the peak area remained almost the same under 2-fold and 5-fold dilution, then decreased sharply with the further increasing AuNP diluent folds. Taking into account the cost, 5-fold dilution of AuNPs was considered optimal for preparing the AuNPs-antibody conjugates for subsequent experiments. As shown in Fig. 2B, the peak area increased up to 2.5 μL, then decreased at 3.0 μL likely due to stereo hindrance between targets and AuNPs-antibody conjugates. Therefore, 2.5 μL of AuNPs-antibody conjugates was considered optimal and used in all further experiments. Fig. 2C shows where the peak area added up to the top at 4 min remained stable between 4 min and 10 min. An accumulation time of 4 min was selected for all subsequent tests. Three types of running buffers were compared as shown in Fig. 2D. The best performance occurred with 4 × SSC +2% BSA +0.05% Tween-20. This buffer offered an appropriate salt ion environment and pH value for the reactions, thus effectively facilitating the detection of rapid-MLPA products on the dual-LFNAB.

### 3.4. Sensitivity

It is very difficult to detect small amounts of nucleic acid, because poor DNA quality is very common due to variations in the abundant DNA in meat, blood, serum, plasma, urine, and other body fluid. Under the optimal conditions described above, 10-fold dilutions of deletion alleles (heterozygous) templates were subjected to the rapid-MLPA and dual-LFNAB cascade to determine the limit of detection. As shown in Fig. 3, the color of test lines was dependent on the amount of target template. For quantitative detection, the limit of detection (LOD) based on 3.3 × standard deviation (SD)/slope of calibration curve was calculated to be approximately 0.4 fM (0.41 fM for wildtype alleles and 0.39 fM for deletion alleles), which is comparable to that of normal-MLPA combined with electrophoresis-based detection assays and electrochemical biosensors (Table S3); however, the proposed assay in this report is considerably quicker and cheaper.

### 3.5. Specificity

To evaluate the interference of undesirable deletion or insertion samples, we tested the specificity of the proposed assay by using six typical model targets: deletion A, deletion B, insertion C, insertion D, insertion E, and random DNA sequences (Table S1). As shown in Fig. 4, the signal of wildtype alleles and deletion alleles (homozygous and heterozygous) was clearly distinct from those produced by other members. No distinct red band was observed on the test lines of dual-LFNABs in the samples absent of wildtype alleles or deletion alleles, as expected. No cross-reactivity with other interference sequences was confirmed by deletion A, deletion B, insertion C, insertion D, or insertion E. In addition, no signal was observed in the random DNA sequences we ran as a control test, indicating negligible nonspecific adsorption of the optimized dual-LFIA. These results altogether indicate that the rapid-MLPA and dual-LFNAB cascade is efficient in the discrimination of one-base deletion.

### 3.6. Reproducibility

Reproducibility is a crucial indicator of practical application for a rapid and low-cost judgment assays. The reproducibility of the proposed approach was determined by testing various sample solutions six times each. As shown in Fig. S7, the coefficients of variation (CV) of the test for 1 pM wildtype alleles and 1 pM deletion alleles (homozygous) were less than 3.0%, which indicates favorable reproducibility. These results are quite promising with respect to testing real gene-editing samples.

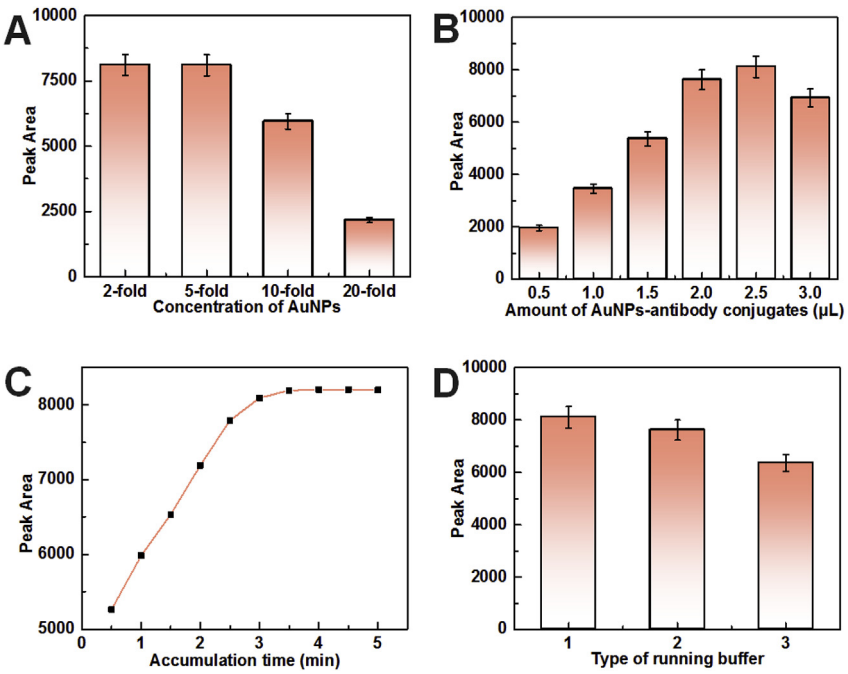


**Fig. 2.** Dual-LFNAB cascade optimization with respect to peak area of test line. (A) Effect of different concentrations of AuNPs: 2-fold, 5-fold, 10-fold, and 20-fold. (B) Effect of different amounts of AuNPs-antibody conjugates: 0.5, 1.0, 1.5, 2.0, 2.5, and 3.0 μL. (C) Effect of different accumulation time: 0.5, 1, 1.5, 2, 2.5, 3, 3.5, 4, and 5 min. (D) Effect of different types of running buffer. 1: 4 × SSC +2% BSA +0.05% Tween-20; 2: 10 mM PBS +2% BSA +0.05% Tween-20; 3: 10 mM Tris-Hcl + 2% BSA +0.05% Tween-20.

Please cite this article in press as: N. Cheng, et al., Rapid and low-cost strategy for detecting genome-editing induced deletion: A single-copy case, Analytica Chimica Acta (2018), https://doi.org/10.1016/j.aca.2018.02.060

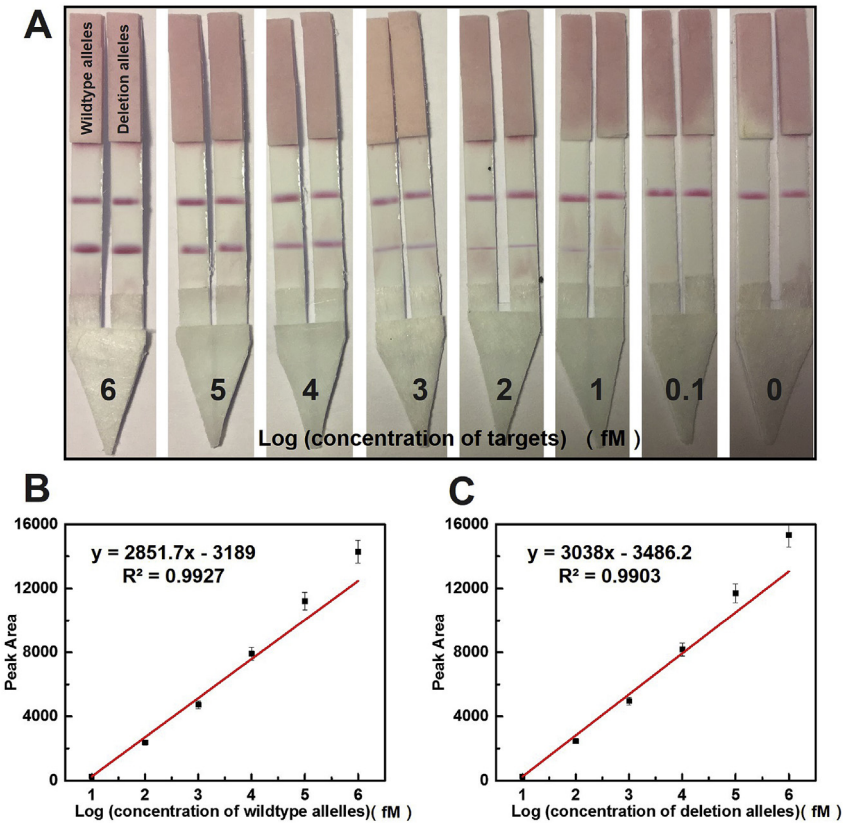


**Fig. 3.** Sensitivity of rapid-MLPA and dual-LFNAB cascade for detection of deletion alleles (heterozygous) with 10-fold dilutions. (A) Typical photo images of dual-LFNABs in the presence of $10^6$, $10^5$, $10^4$, $10^3$, $10^2$, 10, 1, 0.1, and 0 fM of deletion alleles (heterozygous). (B) Calibration curves of peak areas of test lines of wildtype alleles versus target concentrations. (C) Calibration curves of peak areas of test lines of deletion alleles versus target concentrations. Error bars indicate standard deviations of three measurements.

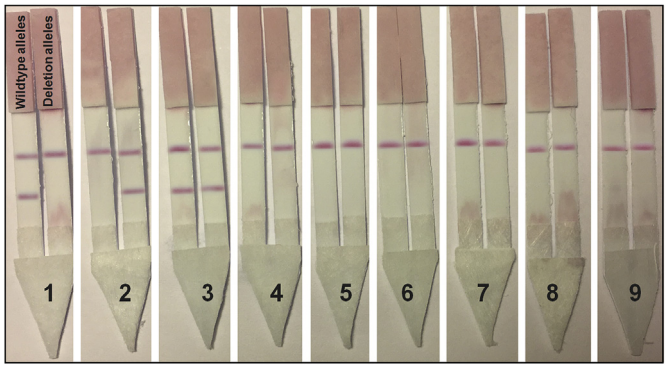


**Fig. 4.** Specificity of rapid-MLPA and dual-LFNAB cascade for determination. (1) Wildtype alleles; (2) Homozygous deletion alleles; (3) Heterozygous deletion alleles; (4) Deletion A; (5) Deletion B; (6) Insertion C; (7) Insertion D; (8) Insertion E; (9) Random DNA. Concentration of all the DNA sequences: 1 pM.

### 3.7. Detection of real samples

We tested two pork samples from two WUZHISHAN pigs to further explore the potential application of the proposed assay in real biological samples. The results we achieved for each sample were compared to the results achieved by PCR-next generation sequencing (gold standard) as summarized in Table 1. There was no significant difference between our assay and the gold standard, further confirming the accuracy and practicality of the proposed approach for detecting genome-editing induced deletion. The above results demonstrate that the device we developed in this study can be applied for the analysis of real biological samples with at least 20-fold shorter assay time and at least 100-fold less assay cost (Table S2). Several different types of samples – wildtype or genome-edited type – may be easily and affordably examined by this method.

## 4. Conclusions and discussions

In conclusion, the rapid-MLPA and dual-LFNAB cascade presented here is a rapid and low-cost system facilitating the detection of genome-editing induced deletion in single-copy cases. Compared to next-generation sequencing analysis, the rapid-MLPA and dual-LFNAB cascade demonstrates at least 20-fold shorter assay time and at least 100-fold less assay cost. The process is initiated by only small amounts of DNA and the results analysis is simple to operate. The proposed dual-LFNAB is a universal platform which can be used to analyze any tag-modified rapid-MLPA products. The cascade is also a universal assay for detecting gene-edited products with specific-site deletion. Taking WUZHISHAN pig as an example, this method is also useful for genotypes analysis of their offspring. One base deletion, as described above, is the most difficult situation to detect – to this effect, a similar strategy can be carried out by minor changes of probes to detect additional deletions. Therefore, the proposed assay may be readily implemented in rapid discrimination between gene-edited mutation and off-target at specific-site during genome-editing. Because this is a specific-site deletion case with single copy in the cell, this assay is an accurate measure of allele targeting frequency. If there are multiple-sites deletion, more primers should be introduced in the system. If there are multiple copies of the target, however, the

Please cite this article in press as: N. Cheng, et al., Rapid and low-cost strategy for detecting genome-editing induced deletion: A single-copy case, Analytica Chimica Acta (2018), https://doi.org/10.1016/j.aca.2018.02.060

**Table 1**
Comparison of rapid-MLPA and dual-LFNAB cascade results to PCR-next generation sequencing results.

| Sample | Rapid-MLPA and dual-LFNAB cascade | | PCR-next generation sequencing | |
|---|---|---|---|---|
| | Image | Result | Image | Result |
| 1 | 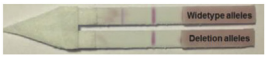  | Wildtype alleles | 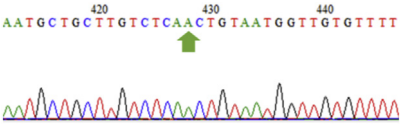  | Wildtype alleles |
| 2 | 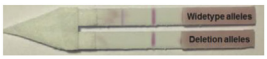  | Homozygous deletion alleles | 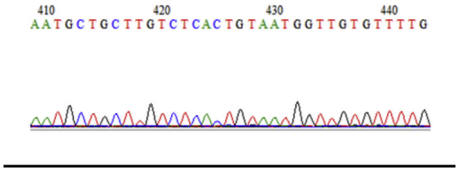  | Homozygous deletion alleles |

situation becomes complicated; this will be focused on our next paper. If there are nucleotide replacement, gene deletion and gene insertion on an unknown site, our proposed method is not applicable.

## Acknowledgement

This work was financially supported by the National GMO Cultivation Major Project of New Varieties (Grant No. 2018ZX08012001) and Natural Science Foundation of China (Grant No.31671922).

## Appendix A. Supplementary data

Supplementary data related to this article can be found at https://doi.org/10.1016/j.aca.2018.02.060.

## References

[1] F.D. Urnov, J.C. Miller, Y.-L. Lee, C.M. Beausejour, J.M. Rock, S. Augustus, A.C. Jamieson, M.H. Porteus, P.D. Gregory, M.C. Holmes, Highly efficient endogenous human gene correction using designed zinc-finger nucleases, Nature 435 (2005) 646.
[2] J.K. Joung, J.D. Sander, TALENs: a widely applicable technology for targeted genome editing, Nat. Rev. Mol. Cell Biol. 14 (2013) 49.
[3] J.A. Doudna, E. Charpentier, The new frontier of genome engineering with CRISPR-Cas9, Science 346 (2014) 1258096.
[4] M. Tabebordbar, K. Zhu, J.K. Cheng, W.L. Chew, J.J. Widrick, W.X. Yan, C. Maesner, E.Y. Wu, R. Xiao, F.A. Ran, In vivo gene editing in dystrophic mouse muscle and muscle stem cells, Science 351 (2016) 407.
[5] R. Barrangou, J.A. Doudna, Applications of CRISPR technologies in research and beyond, Nat. Biotechnol. 34 (2016) 933.
[6] E. Waltz, Gene-edited CRISPR mushroom escapes US regulation, Nature 532 (2016) 293.
[7] E. Waltz, CRISPR-edited crops free to enter market, skip regulation, Nat. Biotechnol. 34 (2016) 582.
[8] S.D. Findlay, K.M. Vincent, J.R. Berman, L.-M. Postovit, A digital PCR-based method for efficient and highly specific screening of genome edited cells, PLoS One 11 (2016) e0153901.
[9] C.C. Bell, G.W. Magor, K.R. Gillinder, A.C. Perkins, A high-throughput screening strategy for detecting CRISPR-Cas9 induced mutations using next-generation sequencing, BMC Genom. 15 (2014) 1002.
[10] Y. Miyaoka, A.H. Chan, B.R. Conklin, Detecting single-nucleotide substitutions induced by genome editing, Cold Spring Harb. Protoc. 2016 (2016) pdb.top.090845.
[11] A. Hendel, E.J. Fine, G. Bao, M.H. Porteus, Quantifying on-and off-target genome editing, Trends Biotechnol. 33 (2015) 132.
[12] J.P. Schouten, C.J. McElgunn, R. Waaijer, D. Zwijnenburg, F. Diepvens, G. Pals, Relative quantification of 40 nucleic acid sequences by multiplex ligation-dependent probe amplification, Nucleic Acids Res. 30 (2002) e57.
[13] J. Na, G.W. Shin, G.Y. Jung, G.Y. Jung, A robust and simple-to-design multiplex DNA methylation assay based on MS-MLPA-CE-SSCP, Analyst 138 (2013) 6969.
[14] J.-B. Yan, M. Xu, C. Xiong, D.-W. Zhou, Z.-R. Ren, Y. Huang, M. Mommersteeg, R. van Beuningen, Y.-T. Wang, S.-X. Liao, Rapid screening for chromosomal aneuploidies using array-MLPA, BMC Med. Genet. 12 (2011) 68.
[15] Y. Shang, P. Zhu, W. Xu, T. Guo, W. Tian, Y. Luo, K. Huang, Single universal primer multiplex ligation-dependent probe amplification with sequencing gel electrophoresis analysis, Anal. Biochem. 443 (2013) 243.
[16] P. Zhang, Y. Liu, Y. Zhang, C. Liu, Z. Wang, Z. Li, Multiplex ligation-dependent probe amplification (MLPA) for ultrasensitive multiplexed microRNA detection using ribonucleotide-modified DNA probes, Chem. Commun. 49 (2013), 10013.
[17] J.L. Acero Sanchez, H. Joda, O.Y. Henry, B.W. Solnestam, L. Kvastad, P.S. Akan, J. Lundeberg, N. Laddach, D. Ramakrishnan, I. Riley, Electrochemical genetic profiling of single cancer cells, Anal. Chem. 89 (6) (2017) 3378−3385.
[18] L. Rooms, G. Vandeweyer, E. Reyniers, K. van Mol, I. de Canck, N. Van der Aa, R. Rossau, R.F. Kooy, Array-based MLPA to detect recurrent copy number variations in patients with idiopathic mental retardation, Am. J. Med. Genet. A 155 (2011) 343.
[19] J.A. Sánchez, O. Henry, H. Joda, B.W. Solnestam, L. Kvastad, E. Johansson, P. Akan, J. Lundeberg, N. Lladach, D. Ramakrishnan, Multiplex PCB-based electrochemical detection of cancer biomarkers using MLPA-barcode approach, Biosens. Bioelectron. 82 (2016) 224.
[20] Y. Chen, N. Cheng, Y. Xu, K. Huang, Y. Luo, W. Xu, Point-of-care and visual detection of P. aeruginosa and its toxin genes by multiple LAMP and lateral flow nucleic acid biosensor, Biosens. Bioelectron. 81 (2016) 317.
[21] N. Cheng, Y. Xu, K. Huang, Y. Chen, Z. Yang, Y. Luo, W. Xu, One-step competitive lateral flow biosensor running on an independent quantification system for smart phones based in-situ detection of trace Hg (II) in tap water, Food Chem. 214 (2017) 169.
[22] W. Xu, N. Cheng, K. Huang, Y. Lin, C. Wang, Y. Xu, L. Zhu, D. Du, Y. Luo, Accurate and easy-to-use assessment of contiguous DNA methylation sites based on proportion competitive quantitative-PCR and lateral flow nucleic acid biosensor, Biosens. Bioelectron. 80 (2016) 654.
[23] N. Cheng, Y. Shang, Y. Xu, L. Zhang, Y. Luo, K. Huang, W. Xu, On-site detection of stacked genetically modified soybean based on event-specific TM-LAMP and a DNAzyme-lateral flow biosensor, Biosens. Bioelectron. 91 (2017) 408.
[24] N. Cheng, Y. Xu, Y. Luo, L. Zhu, Y. Zhang, K. Huang, W. Xu, Specific and relative detection of urinary microRNA signatures in bladder cancer for point-of-care diagnostics, Chem. Commun. 53 (2017) 4222.
[25] F. Chong, X.-r. Li, H.-t. Cui, L. Chuan, L. Xia, X.-h. Tian, D.-k. Pan, Y.-z Luo, Highly efficient generation of GGTA1 knockout pigs using a combination of TALEN mRNA and magnetic beads with somatic cell nuclear transfer, J. Integr. Agr 15 (2016) 1540.
[26] J. Xin, H. Yang, N. Fan, B. Zhao, Z. Ouyang, Z. Liu, Y. Zhao, X. Li, J. Song, Y. Yang, Highly efficient generation of GGTA1 biallelic knockout inbred mini-pigs with TALENs, PLoS One 8 (2013) e84250.
[27] J. Li, J. Macdonald, Multiplexed lateral flow biosensors: technological advances for radically improving point-of-care diagnoses, Biosens. Bioelectron. 83 (2016) 177.